Research in Astron. Astrophys. **2009** Vol. **9** No. **12**, 1303–1316
http://www.raa-journal.org *http://www.iop.org/journals/raa*

***R**esearch in*
***A**stronomy and*
***A**strophysics*

Orbital X-ray modulation study of three supergiant HMXBs

Chetana Jain[1,2], Biswajit Paul[2] and Anjan Dutta[1]

[1] Department of Physics and Astrophysics, University of Delhi, Delhi 110007, India; *chetanajain11@gmail.com*
[2] Raman Research Institute, Sadashivnagar, C. V. Raman Avenue, Bangalore 560080, India

Received 2009 June 27; accepted 2009 August 31

Abstract We present the orbital X-ray modulation study of three high mass X-ray binary systems, IGR J18027−2016, IGR J18483−0311 and IGR J16318−4848, using data obtained with *RXTE*-ASM, *Swift*-BAT and *INTEGRAL*-ISGRI. Using the long term light curves of the eclipsing HMXB IGR J18027−2016, obtained with *Swift*-BAT in the energy range 15−50 keV and *INTEGRAL*-ISGRI in the energy range 22−40 keV, we have determined three new mid eclipse times. The newly determined mid eclipse times together with the known values were used to derive an accurate value of the orbital period of 4.5693(4) d at MJD 52168 and an upper limit of $3.9(1.2)\times10^{-7}$ d d^{-1} on the period derivative. We have also accurately determined an orbital period of 18.5482(88) d for the intermediate system IGR J18483−0311, which displays an unusual behavior and shares many properties with the known SFXTs and persistent supergiant systems. This is a transient source and the outbursts occur intermittently at intervals of 18.55 d. Similarly, in the third supergiant system, IGR J16318−4848, we have found that the outbursts are separated by intervals of 80 d or its multiples, suggesting a possible orbital period.

Key words: X-ray: neutron stars — X-ray binaries: individual (IGR J18027−2016, IGR J18483−0311 and IGR J16318−4848)

1 INTRODUCTION

The INTEernational Gamma-Ray Astrophysics Laboratory *INTEGRAL* was launched in 2002 October (Winkler et al. 2003) and has discovered many new hard X-ray sources during the regular survey of the Galactic center (Revnivtsev et al. 2004; Bird et al. 2007; Kuulkers et al. 2007). In the pre-*INTEGRAL* era, most of the known HMXBs were Be-X-ray binary systems, but the *INTEGRAL* observations have significantly changed the statistics concerning the nature of the companion star of HMXBs. For instance, Liu et al. (2000) have mentioned 54 Be X-ray systems and 7 supergiant X-ray binary systems in their catalog of HMXBs. However, due to the large field of view of the instruments onboard *INTEGRAL* (Lebrun et al. 2003; Ubertini et al. 2003), and the high sensitivity to hard X-rays, several new HMXBs have been discovered and the proportion of supergiant systems has increased drastically. It has particularly revealed many new HMXBs which are obscured by the dense and highly absorbing circumstellar wind of the companion, because of which these X-ray sources are not observable at low energies. Bird et al. (2007) identified 68 HMXBs in their third IBIS/ISGRI soft γ-ray survey catalog. Out of these, 24 systems were identified as Be X-ray systems and 19 as supergiants. In about 5 years since its launch, *INTEGRAL* has revealed two distinct classes of supergiant X-ray binary systems. The first class includes obscured persistent sources (Kuulkers 2005) and the second class includes sources displaying a short transitory nature (Supergiant Fast X-ray Transients, SFXTs) with outbursts lasting for a few hours

(Negueruela et al. 2006; Sguera et al. 2005, 2006). Further, several persistent low luminosity, slow X-ray pulsators have also been identified, some of which belong to HMXB systems (Kaur et al. 2009).

Figure 1 shows the orbital period distribution of the different sub-classes of high mass X-ray binaries. We have categorized the distribution into Be-star systems, the SFXTs, the persistent supergiant systems and the obscured systems. Only orbital periods of those HMXBs mentioned in the HMXB catalog by Liu et al. (2007) are shown. It is clear from the figure that the orbital periods in the Be-star systems range between 12−262 d, whereas the orbital periods of supergiant systems are relatively shorter. The orbital periods in these systems are mostly less than 15 d, except for one system having an orbital period of 42 d. Amongst the SFXTs listed in the catalog, the orbital period is known in six systems and it varies over a wide range of 3.3−165 d. The obscured sources tend to have small orbital periods with the widest known orbital period of about 13 d. The orbital periods of the three sources studied in this work are marked with a "plus" sign. The first source is an intermediate SFXT having an orbital period of about 18 d. The second source is a supergiant HMXB having an orbital period of 4.5693 d, whereas the third one is a highly obscured system. As detailed later, we have determined a possible orbital period of ∼80 d in this source. If the inferred outburst period is indeed its orbital period, then this obscured system would have a period significantly longer (by more than a factor of 4) than any of the previously determined periods of systems in this category.

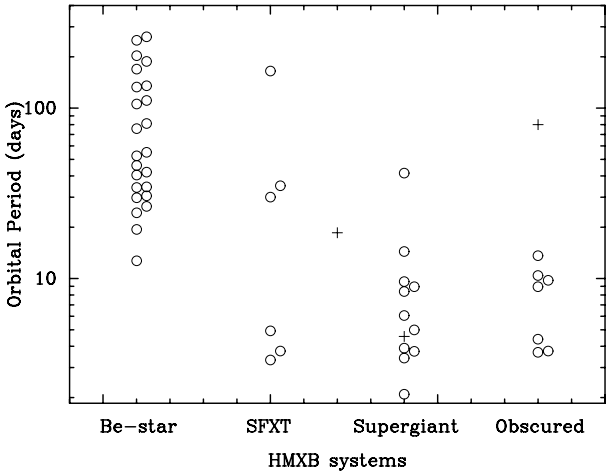

Fig. 1 Orbital period distribution in high mass X-ray binaries categorized into the Be-star systems, the SFXTs, the persistent supergiants and the obscured sources. The "+" indicates the orbital period of the three systems studied in the present work.

We have carried out orbital modulation studies of bright *INTEGRAL* sources and have discovered a very short orbital period in one source, SFXT IGR J16479−4514 (Jain et al. 2009). Here, we present results from three of the brightest *INTEGRAL* sources, IGR J18027−2016, IGR J18483−0311 and IGR J16318−4848. These systems have a late O/early B type supergiant companion and are highly absorbed sources. The optical counterparts of the sources IGR J18027−2016 and IGR J18483−0311 were first identified spectroscopically by Masetti et al. (2008). While IGR J18027−2016 and IGR J18483−0311 are pulsars, the nature of the compact object in IGR J16318−4848 is not yet known in spite of extensive observations with different observatories. IGR J18027−2016 is an eclipsing high mass X-ray binary consisting of a neutron star spinning with a period of 139 s. The eclipses provide a good fiducial timing marker for precise determination of the orbital evolution. IGR J18483−0311 is an intermediate system whose position on the Corbet diagram (Corbet 1986) indicates that it is most likely a Be system, but the periodic fast X-ray transient activity observed in this system is typical of an SFXT system. It is therefore important to determine its orbital parameters. IGR J16318−4848 is one of the most absorbed

Galactic sources known with an enormously high column density. A study of orbital modulation in all these systems is important to understand the mechanism for the short and long duration outbursts and is also useful in planning future orbital phase dependent observations.

IGR J18027−2016 is spatially associated with the X-ray pulsar SAX J1802.7−2017 (Augello et al. 2003) which was serendipitously discovered during a *Beppo*-SAX observation of the LMXB GX 9+1 in 2001 September. It is an eclipsing HMXB system and harbors an X-ray pulsar accreting matter from the stellar wind of the companion star, which is a late O/early B-type supergiant with a mass of 18.8−29.3 $M_{\odot}$ (Hill et al. 2005). From the *Beppo*-SAX observations, Augello et al. (2003) determined a pulse period of 139.612 s and from the pulse arrival time analysis, they determined an orbital period of ∼4.6 d. It was later confirmed by Hill et al. (2005), who determined an orbital period of 4.5696(9) d from the eclipse timing measurement of the ISGRI data. They also determined a projected semimajor axis ($a_x \sin i$) of 68 lt-s and a mass function of 16 $M_{\odot}$, from which they concluded the mass of the donor to be 18.8−29.3 $M_{\odot}$ and a radius of 15.0−23.4 $R_{\odot}$. Spectral analysis with *XMM-Newton* and *INTEGRAL-ISGRI* indicates a strong intrinsic absorption with a hydrogen column density $N_{\rm H}$ of 6.8× 10^{22} cm^{-2} (Hill et al. 2005). Lutovinov et al. (2005) fitted the 18−60 keV spectrum with a powerlaw along with an exponential cutoff at high energies ($E_{\rm c} \sim 18$ keV).

IGR J18483−0311 was discovered with *INTEGRAL* during a survey of the Galactic plane in 2003 April (Chernyakova et al. 2003). An average flux of ∼10 mCrab in the 15−40 keV range was observed, which decreased to 5 mCrab in the 40−100 keV energy range. IGR J18483−0311 is a high mass X-ray binary with an early B-type supergiant companion star (Rahoui et al. 2008). From the timing analysis of the *RXTE*-ASM light curve, Levine & Corbet (2006) reported a 18.55(5) d orbital period and 21 s X-ray pulsations were reported by Sguera et al. (2007). The source displays an unusual behavior and shares many properties with the known SFXTs and persistent supergiant systems. Association with a B0.5Ia supergiant companion star (Rahoui et al. 2008) and fast X-ray transient activity (Sguera et al. 2007) indicates that the system could be an SFXT. However, the outbursts last for a few days, in contrast to the outbursts of a few hours seen in other well known SFXTs (Sguera et al. 2007). The quiescent emission level is also higher in IGR J18483−0311, yielding an $L_{\rm max}/L_{\rm min}$ ratio of ∼10^3, whereas, in SFXTs, the ratio is $10^4 - 10^5$. The system is therefore considered to be an "intermediate" SFXT. The 3−50 keV spectra is well fitted by an absorbed powerlaw with a photon index of 1.4 and a cutoff at 22 keV. A high intrinsic absorption is also seen with a column density, $N_{\rm H}$, of 9 ×10^{22} cm^{-2}. Spectra during the outbursts are well fitted by an absorbed bremsstrahlung with $N_{\rm H}$ of 7.5×10^{22} cm^{-2} and kT ∼ 21.5 keV (Sguera et al. 2007).

IGR J16318−4848 is one of the highly obscured Galactic X-ray sources discovered by *INTEGRAL* (Courvoisier et al. 2003) and followed up by the *XMM-Newton* observatory which accurately localized its position (de Plaa et al. 2003; Schartel et al. 2003). A flux of 50−100 mCrab was observed in the 15−40 keV energy band with a significant variability on timescales of more than 1000 s (Walter et al. 2003). Observations made with the *XMM-Newton* revealed the presence of strong Fe-K$_{\alpha}$, Fe-K$_{\beta}$ and Ni-K$_{\alpha}$ emission lines (Schartel et al. 2003; de Plaa et al. 2003), along with a highly absorbed powerlaw (Γ ∼1.7−2.1) continuum (Matt & Guainazzi 2003). The IR spectrum is also rich in emission lines and various orders of H, He I and He II (Kaplan et al. 2006). IGR J16318−4848 is surrounded by dense circumstellar material and powered by accretion from a stellar wind (Revnivtsev et al. 2003; Filliatre & Chaty 2004). From the archived *ASCA* observations, Revnivtsev et al. (2003) determined an enormously high column density, $N_{\rm H} \simeq 10^{24}$ cm^{-2}, due to which, the source is not observable at energies below 4 keV.

We report the timing analysis of these three bright supergiant systems, IGR J18027−2016, IGR J18483−0311 and IGR J16318−4848. Using the data obtained from *Swift*-BAT and *INTEGRAL*-ISGRI, we have determined the orbital periods of IGR J18027−2016 and IGR J18483−0311. We have also discovered an 80 d periodicity in the occurrence of outbursts in IGR J16318−4848, which is possibly indicative of a binary orbital period.

2 OBSERVATIONS AND ANALYSIS

We have used data obtained with instruments onboard the Rossi X-ray Timing Explorer (*RXTE*), the *Swift* Gamma Ray Burst Explorer and the INTErnational Gamma-Ray Astrophysics Laboratory (*INTEGRAL*). The three sources were regularly monitored by the All Sky Monitor (ASM) onboard the *RXTE*. The ASM data used for the present work covered the time span from MJD 50088 to MJD 54860. The 15−50 keV light curves of IGR J18027−2016, IGR J18483−0311 and IGR J16318−4848 were obtained from the Burst Alert Telescope (BAT; Barthelmy et al. 2005) onboard the *Swift* observatory. The observations covered the time range from MJD 53413 to MJD 54867. For all the three sources, the 22−40 keV long term *INTEGRAL*-ISGRI light curve spanned ∼1350 d.

IGR J18027−2016: The long term *Swift*-BAT, *INTEGRAL*-ISGRI and *RXTE*-ASM light curves of IGR J18027−2016 were corrected for the earth's motion using the *earth2sun* tool of the HEASARC software package "Ftools" ver6.5.1. We searched for the orbital period using the ftool - *efsearch*, which folds the light curve with a large number of trial periods around an approximate period. Figure 2 shows the *efsearch* result on the light curve of IGR J18027−2016.

The top panel shows the result of the period search on the long term *Swift*-BAT light curve. The peak here corresponds to the periodicity in the light curve. The inset figure is the expanded view around the peak. A gaussian fit around the peak gave the gaussian center as 394 793(103) s (4.5693(11) d). The *efsearch* result of the *INTEGRAL* data, over the same range as in *Swift*-BAT, is shown in the second panel. The main peak corresponds to a period of 395 056(210) s (4.5723(24) d). It should be noted that the present *INTEGRAL* dataset is longer than that analyzed by Hill et al. (2005), who determined a period of 4.570(3) d using the ISGRI data spanning ∼ 417 d. The *INTEGRAL* data used in the present work covered the time range from MJD 52 698 to MJD 54041. The third panel shows the *efsearch* result on the 5−12 keV *RXTE*-ASM light curve. A peak is present but with a poor significance. The peak corresponds to a period of 394 805(185) s (4.5695(21) d).

We have also confirmed the periodicity in the light curves of IGR J18027−2016, using the Lomb-Scargle periodogram method by means of the fast implementation of the Press & Rybicki (1989) and Scargle (1982) technique. Figure 3 shows the periodogram generated using the *Swift*-BAT, *INTEGRAL*-ISGRI and *RXTE*-ASM light curves.

As seen in Figure 3, a clear peak is present in the periodogram generated from the *Swift* and *INTEGRAL* light curves. However, periodicity could not be confirmed from the *RXTE*-ASM observations. The power spectrum in the case of the *Swift*-BAT and *INTEGRAL*-ISGRI data peaks at 0.218 d^{-1}, which corresponds to a periodicity of 4.5871 d. This result is in sync with the values determined by the *efsearch* analysis and those reported by Hill et al. (2005). The significance of these peaks was confirmed by a randomization test. For both *Swift*-BAT and *INTEGRAL*-ISGRI light curves, the time stamps of the observed count rates were randomly shuffled and a periodogram was generated from the resulting time series. We simulated 10 000 light curves and determined the maximum power for both cases. As shown in Figure 3, the horizontal lines in the top two panels show the significance level. The dotted and dashed lines respectively show the 99.9% and 99% significance power among the randomized light curves. This implies that a peak power of 281 and 61 in the original *Swift*-BAT and *INTEGRAL*-ISGRI periodograms is unlikely to occur by chance and therefore the period detection is significant.

To determine the long term orbital solution, we folded the *Swift*-BAT, *INTEGRAL*-ISGRI and *RXTE*-ASM light curves in 16 phasebins with a period of 394 805 s. The folded light curves are shown in Figure 4. A sharp eclipse is clearly seen in the folded *Swift*-BAT light curve. The eclipse lasts for ∼ 0.2 orbital phase. A clear eclipse is also seen in the folded *INTEGRAL*-ISGRI light curve but it is not as sharp when compared to the eclipse seen in the folded *Swift*-BAT light curve. The eclipse detection in the folded *RXTE*-ASM light curve is not significant, but we emphasize that it occurs at the same phase as seen in the other two observations. We fitted a gaussian to the eclipse phase and the center of the best fit gaussian gives the mid eclipse time for that observation. From the folded *Swift*-BAT light curve, we determined an eclipse half width of 0.1923 orbital phase. This implies an eclipse half angle of 0.604 radians. The mass of the companion star is known to lie within a range of 19−29 $M_\odot$. Therefore,

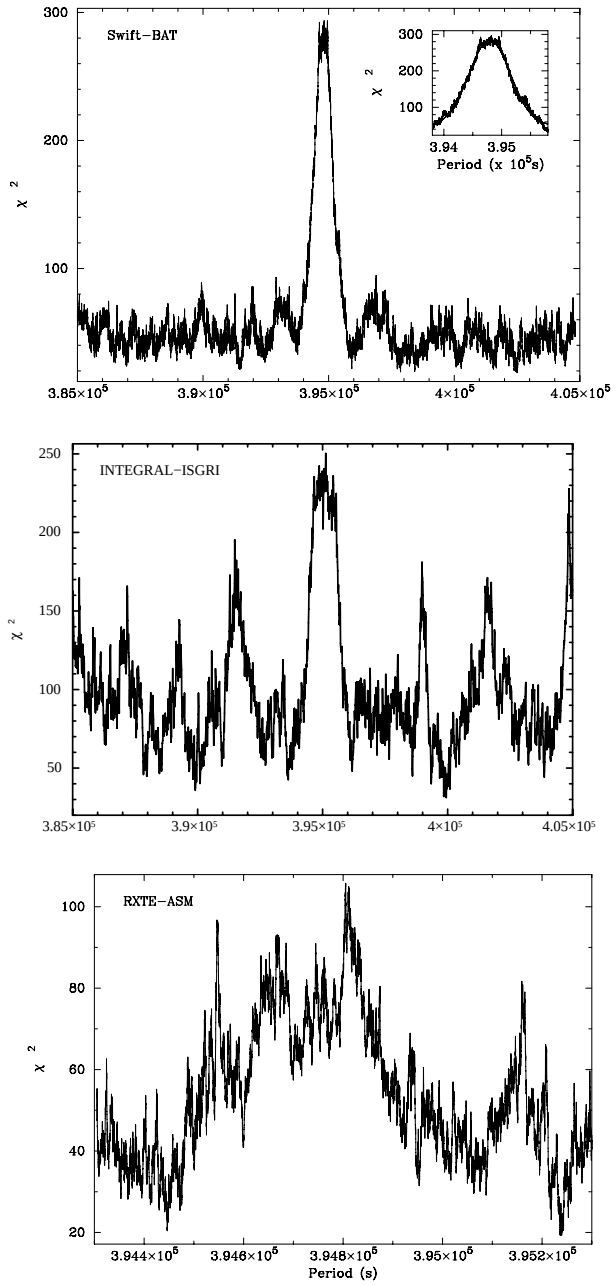

Fig. 2 Results from *efsearch* applied to the light curve of IGR J18027−2016. The top panel shows the result from the *Swift*-BAT observations and the inset figure shows the expanded view around the peak. The solid line represents the best fit gaussian curve with the center at 394793(103) s. The second and third panels show the *efsearch* results from the *INTEGRAL*-ISGRI and *RXTE*-ASM light curves. The peak in the *INTEGRAL*-ISGRI result corresponds to a period of 395056(210) s, while from the *RXTE*-ASM data, we determined a period of 394805(185) s.

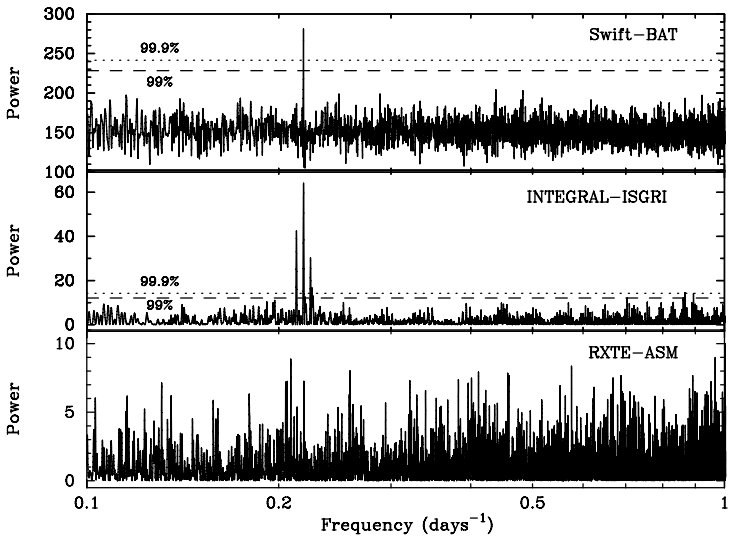

Fig. 3 Lomb-Scargle periodogram generated from the *Swift*-BAT, *INTEGRAL*-ISGRI and *RXTE*-ASM light curves of IGR J18027−2016. The highest peak in the top and the middle panels correspond to a frequency of 0.218 d^{-1}, i.e. a period of 4.5871 d.

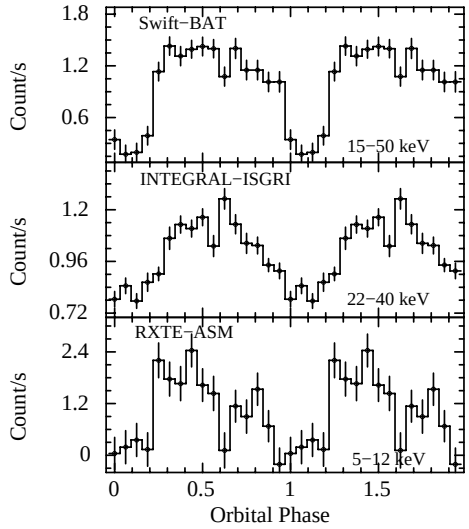

Fig. 4 Light curve of IGR J18027−2016 folded in 16 bins with a period of 394 805 s. The folded light curves of *Swift*-BAT, *INTEGRAL*-ISGRI and *RXTE*-ASM observations are shown in the top, middle and bottom panels respectively.

assuming a canonical mass of 1.4 $M_\odot$ for the neutron star, the lower limit of the companion star radius will lie in the range of 16.4−24.7 $R_\odot$.

Table 1 gives a log of the mid eclipse times determined from each observation.

We determined two mid eclipse times from the *Swift*-BAT data and one from the *INTEGRAL*-ISGRI data. The eclipse seen in the *RXTE*-ASM light curve is not sharp and therefore the determination of the

Table 1 X-ray Mid-eclipse Times of IGR J18027−2016

Cycle	Mid eclipse time (MJD)	Uncertainty (d)	Satellite
0†	52168.26	0.04	*Beppo*-SAX
68	52478.78	0.12	*RXTE*-ASM
167†	52931.37	0.04	*INTEGRAL*-ISGRI
239	53260.37	0.07	*INTEGRAL*-ISGRI
352	53776.82	0.07	*Swift*-BAT
511	54503.38	0.07	*Swift*-BAT

† Reported by Hill et al. (2005).

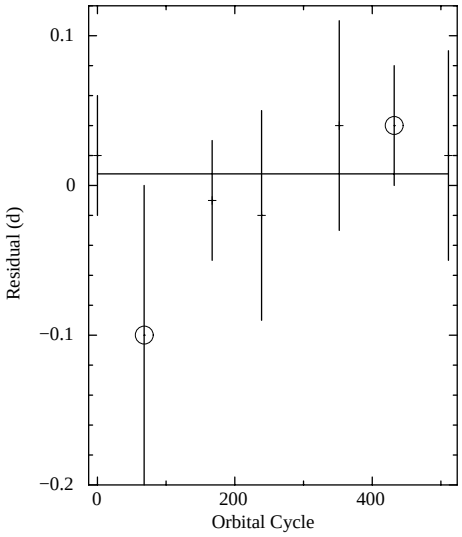

Fig. 5 Mid eclipse time residuals of IGR J18027−2016 are plotted as a function of the orbital cycle, relative to the best fit linear ephemeris ($P_{\rm orb}$ = 4.5693 d at MJD 52168). The mid eclipse times are tabulated in Table 1. The "O" represents the *RXTE*-ASM and average *Swift*-BAT, respectively.

mid eclipse time involves a significant error. We then combined these newly determined mid eclipse times with the known values and fitted a quadratic model to the ephemeris history. We determined an orbital period ($P_{\rm orb}$) of 394 787(34) s (4.5693(4) d) and a period derivative of $3.9(1.2)\times10^{-7}$ d d^{-1} at MJD 52 168. We then subtracted the best fit linear component from the ephemeris history and the residual is plotted in Figure 5. There are only a few mid eclipse times reported for this source, therefore, it is not possible to accurately determine the orbital evolution of this binary system. However, it should be noted that the period is indeed evolving and, probably, future observations of the source can lead to the determination of the orbital evolution in this system. In particular, since this is an eclipsing system, the optical measurements of the companion star can be useful in placing a constraint on the rate of mass loss from the donor star.

IGR J18483−0311: The *efsearch* period search result of the long term *Swift*-BAT, *INTEGRAL*-ISGRI and *RXTE*-ASM light curves of IGR J18483−0311 are shown in Figure 6. Clear peaks are seen in all of the three results. A gaussian was fitted around the peak in the *Swift*-BAT period search results (inset figure in the top panel) and the peak center determined. An orbital period of 1 602 796(2268) s (18.550(26) d) was determined. The peak in the *efsearch* result of the 22−40 keV *INTEGRAL*-ISGRI and 5−12 keV *RXTE*-ASM light curves corresponds to 1 600 227(2989) s (18.521(34) d) and 1 602 571(767) s (18.5482(88) d), respectively. These results are an improvement over the results ob-

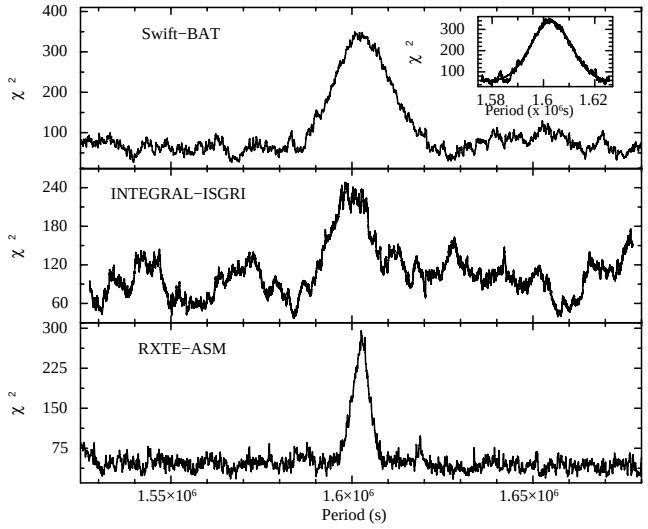

Fig. 6 Results from *efsearch* of the light curve of IGR J18483−0311. The top, middle and bottom panels show the result from the *Swift*-BAT, *INTEGRAL*-ISGRI and *RXTE*-ASM observations, respectively. The inset figure in the top panel shows the expanded view around the peak determined from the *Swift*-BAT observations. The solid line represents the best fit gaussian curve with the center at 18.550(26) d. The peaks in the *INTEGRAL*-ISGRI and *RXTE*-ASM results respectively correspond to a period of 18.521(34) d and 18.5482(88) d.

tained by Sguera et al. (2007), who analyzed $\sim$ 1 142 d of data from the *INTEGRAL* observations and determined an orbital period of 18.52 d. Whereas, the present result is more complete with the *INTEGRAL* data covering the time range from MJD 52 704 to MJD 54 053.

IGR J18483−0311 is a bursting source and, therefore, initially we could not determine an accurate period from the *efsearch* analysis of the entire *INTEGRAL* light curve. However, after the removal of 5 σ bursts (as explained later), we determined the orbital period accurately. We have confirmed the periodicity in the long term *Swift*-BAT and *RXTE*-ASM light curves by using the Lomb-Scargle periodogram technique as mentioned in the case of IGR J18027−2016.

As shown in Figure 7, the peak in the Lomb-Scargle periodogram of the *Swift*-BAT light curve corresponds to 0.0538 d^{-1}, i.e. a period of 18.5873 d. Similarly, from the *RXTE*-ASM light curve (Fig. 7, bottom panel) a period of 18.7617 d has been found. The dotted and the dashed horizontal lines in Figure 7 correspond to a 99.9% and 99% significance level as determined from the randomization test explained before. The *Swift*-BAT, *INTEGRAL*-ISGRI and *RXTE*-ASM light curves were folded into 32 phasebins with a period of 1 602 571 s and are shown in Figure 8.

Clear peaks are seen in all the three folded light curves. The folded light curve shows that the source is inactive for about half the orbit.

IGR J18483−0311 is a transient source and many outbursts have been recorded by the instruments onboard *INTEGRAL*. Figure 9 shows the long term *INTEGRAL*-ISGRI light curve binned with an orbital period of 18.5482 d. The bottom panel of the same figure shows the long term light curve binned with a period one-sixteenth of the orbital period.

Large variations, akin to the SFXT outbursts, are seen in the bottom panel compared to the light curve shown in the top panel. To determine their phase occurrence, we took the light curve binned with 1.1592 d and, assuming a uniform exposure throughout the observation, we divided the signal count rate by the error associated with it. The resulting light curve is shown in Figure 10 (left panel). We then took the outbursts above the 5 σ and 10 σ level and, considering an orbital period of 18.5482 d, we determined their phase of occurrence with respect to the most intense outburst. A histogram of the

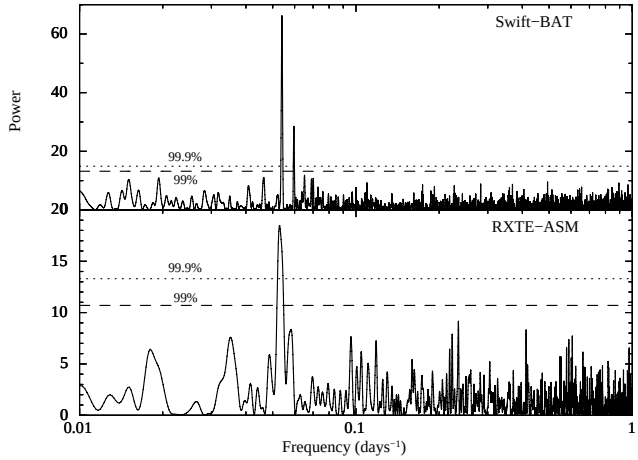

Fig. 7 Lomb-Scargle periodograms generated from the *Swift*-BAT and *RXTE*-ASM light curves of IGR J18483−0311 are respectively shown in the top and the bottom panel. The peak in the top panel corresponds to a frequency of $0.0538\,\mathrm{d}^{-1}$, i.e. a period of 18.5873 d. The peak in the periodogram generated from the *RXTE* data corresponds to a frequency of $0.0533\,\mathrm{d}^{-1}$, i.e. a period of 18.7617 d.

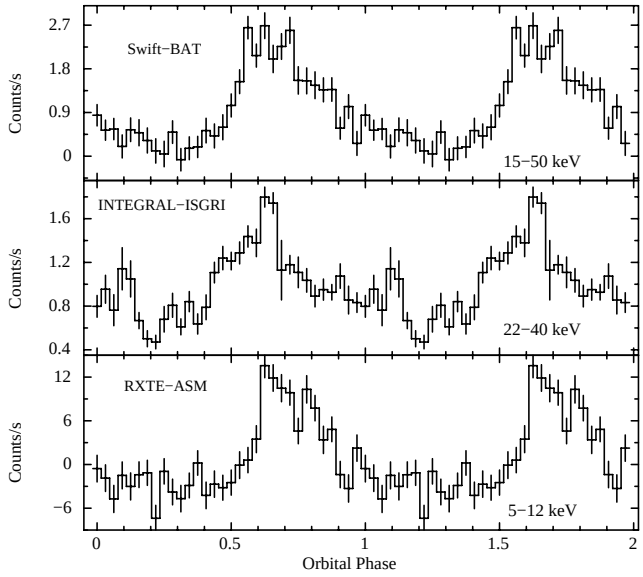

Fig. 8 Light curve of IGR J18483−0311 folded into 32 bins with a period of 1 602 571 s. The top, middle and bottom panels, respectively show the folded light curves of the *Swift*-BAT, *INTEGRAL*-ISGRI and *RXTE*-ASM observations.

number of outbursts in each orbital phase was created. It is shown in the right panel of Figure 10. The solid curve in the histogram corresponds to the outburst above the $10\,\sigma$ level and the dotted curve is for the $5\,\sigma$ level. As can be seen in the figure, most of the outbursts occur at the same phase as the referenced "most intense" outburst. A few outbursts do also occur at other phases, but this result confirms the periodicity in the occurrence of outbursts.

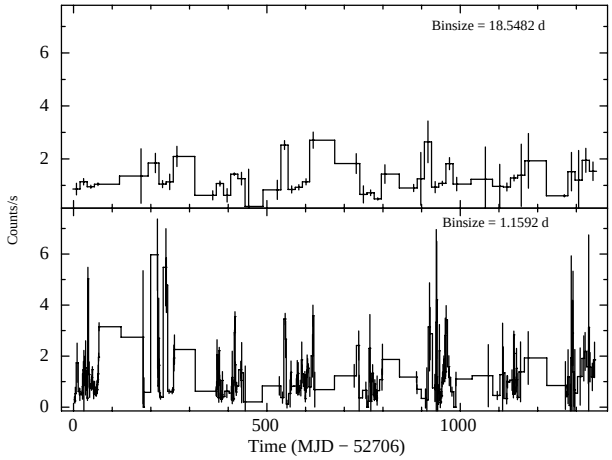

Fig. 9 Long term light curve of IGR J18483−0311, binned with binsizes of 18.5482 d and 1.1592 d.

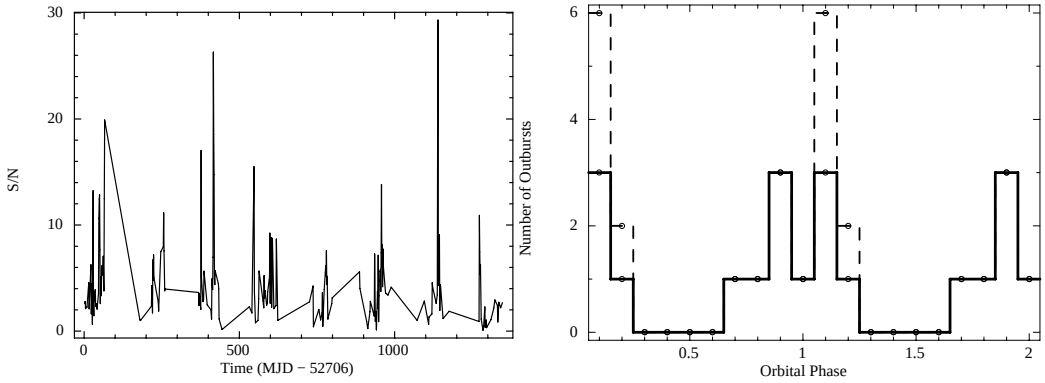

Fig. 10 *Swift*-BAT light curve of IGR J18483−0311, binned with a binsize of 1.1592 d. The count rate was divided by the error. The right panel shows the histogram of the number of outbursts with respect to the orbital phase. The dashed line shows the number of outbursts above the $5\,\sigma$ level and the solid line shows the number of outbursts above the $10\,\sigma$ level.

After the removal of the $5\,\sigma$ bursts, we searched for an orbital period in the *INTEGRAL* data and the *efsearch* result is shown in Figure 6 (middle panel). The folded *INTEGRAL* light curve, after the removal of the $5\,\sigma$ outbursts, which is shown in Figure 8 (middle panel). The profile is similar to the folded profile obtained from the *Swift*-BAT and the *RXTE*-ASM light curves.

IGR J16318−4848: As done in the case of IGR J18027−2016 and IGR J18483−0311, the long term *Swift*-BAT, *INTEGRAL*-ISGRI and *RXTE*-ASM light curves were first corrected for the earth's motion and the periodicity was searched using the ftool *efsearch*. The period search results are shown in Figure 11.

The top panel shows the *efsearch* result from the *Swift*-BAT light curve and a peak is seen near $\sim 7 \times 10^6$ s. The period search analysis in IGR J16318−4848 is being reported for the first time, therefore, we have searched for a period over a wide range of trial periods. The inset figure is the expanded view around the peak, to which we fit a gaussian model. We obtained the best fit gaussian center as 6 931 624(1202) s (80.227(14) d). The detection significance of periodicity from the *INTEGRAL* and

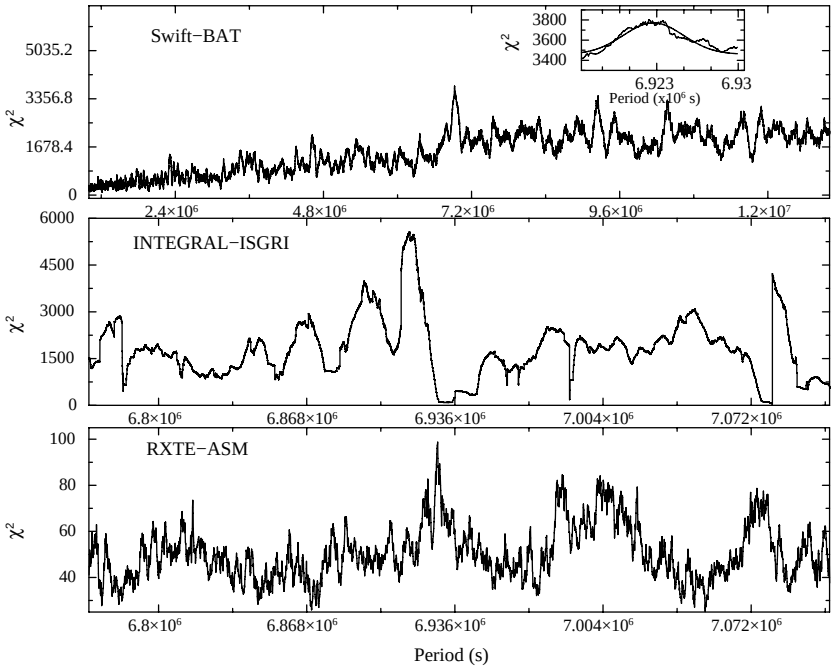

Fig. 11 Results from *efsearch* on the light curve of IGR J16318−4848. The top panel shows the result from the *Swift*-BAT observations, over a wide range of trial periods. The inset figure shows the expanded view around the peak determined from the *Swift*-BAT dataset. The solid line represents the best fit gaussian curve with the center at 80.227(14) d. The middle and the bottom panels show the *efsearch* result near the peak from the *INTEGRAL* and *RXTE*-ASM data. The peaks correspond to 80.045(21) d and 80.198(22) d, respectively.

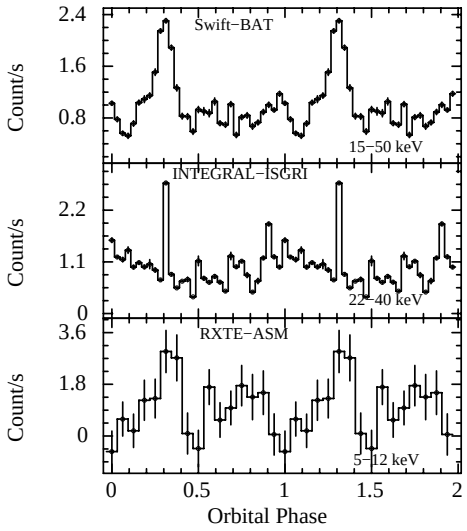

Fig. 12 Folded *Swift*-BAT, *INTEGRAL*-ISGRI and *RXTE*-ASM light curves of IGR J16318−4848. The light curves were folded with the respective best period determined in each case.

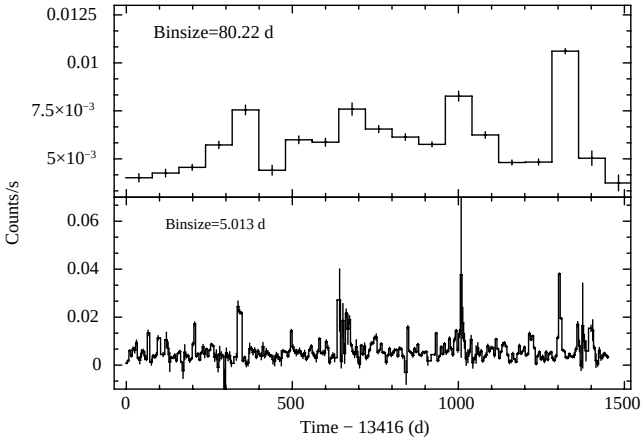

Fig. 13 Long term light curves of IGR J16318−4848, binned with binsizes of 80.22 d and 5.013 d.

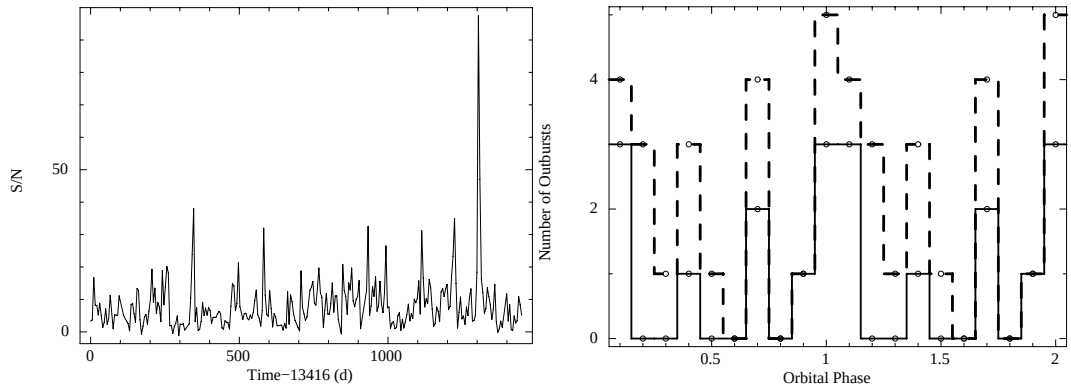

Fig. 14 *Swift*-BAT light curve of IGR J16318−4848, binned with a binsize of 5.013 d. The count rate was divided by the error. The right panel shows the histogram of the number of outbursts with respect to the orbital phase. The dashed line shows the number of outbursts greater than 15 σ and the solid line shows the number of outbursts greater than the 20 σ level.

RXTE observations is very small, but we do detect a peak at 6 915 874(1808) s (80.045(21) d) and 6 929 084(1912) s (80.198(22) d), respectively. We tried to confirm the periodicity using the Lomb-Scargle periodogram technique as done above for the other two sources, but we could not detect a significant peak.

Figure 12 shows the folded *Swift*-BAT, *INTEGRAL*-ISGRI and *RXTE*-ASM light curves of IGR J16318–4848. The light curves were folded with the respective best period determined in each case. We have done the rest of the analysis with the *Swift*-BAT light curve, which has the best statistics amongst the three observations.

A clear peak is seen in the folded light curve, along with small secondary peaks. The main peak lasts for about 0.2 orbital phase. Figure 13 shows the *Swift*-BAT light curve binned with a binsize of 80.22 d. The bottom panel of the same figure shows the light curves binned with a binsize one-sixteenth of 80.22 d. An intense outburst near the end of the observation clearly stands out and the peak observed in the folded orbital light curve could be dominated by this.

To check this, we applied a similar analysis as done above for IGR J18483−0311. We divided the signal count rate by the error in rate determination for the light curve binned with 5.013 d (shown

in Fig. 14 (left panel)). We then took the outbursts above the $15\,\sigma$ and $20\,\sigma$ level and, considering an orbital period of 80 d, we determined the phase of occurrence of outbursts with respect to the most intense outburst. The right panel of Figure 14 shows the histogram of the number of outbursts in each phase. Most of the outbursts occur around an orbital phase of 0.1, with occasional outbursts at phases about 0.4 and 0.7. It implies that, though the outbursts occur with a periodicity of ~ 80 d, there are three different orbital phases at which they occur.

3 DISCUSSION

Using the long term *Swift*-BAT, *INTEGRAL*-ISGRI and *RXTE*-ASM data of IGR J18027−2016, we have determined an accurate value of the orbital period of 4.5693(4) d. From the *Swift*-BAT and *RXTE*-ASM data, we have accurately determined an orbital period of 18.5482(88) d for IGR J18483−0311 and have found that the outbursts occur intermittently at intervals of ~ 18.55 d. We have also found an ~ 80 d periodicity in the occurrence of outbursts from IGR J16318−4848.

All the three sources, IGR J18027−2016, IGR J18483−0311 and IGR J16318−4848, studied in the present work, are bright supergiant High Mass X-ray Binaries which accrete material through the stellar wind of a late O/early B-type supergiant companion. The classical supergiant systems have small and circular orbits, as compared to relatively larger orbits found in Supergiant Fast X-ray Transients. However, there are exceptions to this. Recently, Jain et al. (2009) determined a 3.32 d orbital period for the SFXT system IGR J16479−4514, which is smaller than that known in other SFXTs, IGR J11215−5952 (165 d: Romano et al. 2007; Sidoli et al. 2007) and SAX J1818.6−1703 (30 d: Bird et al. 2009). An orbital period of 4.56 d for IGR J18027−2016 is well within the expected range for supergiant systems, but an orbital period of 18.5508 d, determined for IGR J18483−0311, is somewhat more than that expected from a supergiant system. IGR J18483−0311 is active for about half the orbital cycle. The quiescent emission level in IGR J18483−0311 is also higher (Sguera et al. 2007). All this implies that the source is an intermediate system between classical supergiants and SFXTs.

IGR J16318−4848 is a highly absorbed source with a hydrogen column density of $N_{\rm H} \simeq 10^{24}\,{\rm cm}^{-2}$. The presence of strong absorption shows that the compact object must be embedded in a dense circumstellar envelope, originating from the accretion of stellar winds. In several HMXBs, the orbital periods have been determined either through the timing analysis of the X-ray data (for example, IGR J16479−4514: Jain et al. 2009; IGR J17544−2619: Clark et al. 2009; IGR J17252−3616: Zurita Heras et al. 2006) or through the timing of the recurrent outbursts (for example IGR J11215−5952: Sidoli et al. 2007; SAX J1818.6−1703: Sidoli et al. 2009). We have studied the periodicity in the occurrence of outbursts in this system. The periodicity of ~ 80 d in the outburst behavior most likely represents the orbital period of the binary system and is a key diagnostic for studying the geometry of the system.

Several models have been proposed to explain the occurrence of periodic outbursts in the supergiant systems. In't Zand (2005) suggested the "clumpy winds" model, according to which the wind from the donor star is composed of dense clumps with a mass on the order of $10^{19} - 10^{20}$ g (Howk et al. 2000). The neutron star accretes from the wind of the supergiant at different rates depending on the wind density and short flares that occur due to the episodic accretion of clumps from the massive winds. Negueruela et al. (2008) suggested that outbursts occur due to the accretion of clumps from the spherical wind. They proposed that the orbits of these systems are large and the wind clump density is small. The outbursts in IGR J16318−4848 have been observed to occur at different orbital phases. The pattern of the X-ray outbursts depends on the size, eccentricity and the orientation of the orbit. Sidoli et al. (2007) proposed that the supergiant wind has an "equatorial disk" component in addition to the spherically symmetric polar component. Outbursts occur when the neutron star crosses the equatorial disk component at the periastron, which is denser than the polar wind component. The neutron star can cross the disk twice depending on the truncation of the disk, and its orientation and inclination with respect to the orbital plane.

In view of the results presented above, we point out that more sensitive and frequent monitoring of all the three sources is required in order to understand them in detail, especially in the case of IGR

J18027−2016, which shows clear eclipses which can be used to time mark the orbital modulation and determine the orbital evolution in the system, if any. Using longer data sets, we have been able to determine the orbital period of IGR J18483−0311 with greater accuracy. Regular monitoring of the absorbed source IGR J16318−4848 is important in order to detect the orbital period with confidence.

Acknowledgements We thank the anonymous referee for some useful comments to improve the manuscript. We also thank the *Swift*-BAT and *RXTE*-ASM teams for the provision of the data.

References

Augello, G., Iaria, R., Robba, N. R., Di Salvo, T., Burderi, L., Lavagetto, G., & Stella, L. 2003, ApJ, 596, L63
Barthelmy, S. D., Barbier, L. M., Cummings, J. R., et al. 2005, Space Science Reviews, 120, 143
Bird, A. J., Malizia, A., Bazzano, A., et al. 2007, ApJS, 170, 175
Bird, A. J., Bazzano, A., Hill, A. B., McBride, V. A., Sguera, V., Shaw, S. E., & Watkins, H. J. 2009, MNRAS, 393, L11
Chernyakova, M., Lutovinov, A., Capitanio, F., Lund, N., & Gehrels, N. 2003, ATel, 157, 1
Clark, D. J., Hill, A. B., Bird, A. J., McBride, V. A., Scaringi, S., & Dean, A. J. 2009, arXiv:0908.1041
Corbet, R. H. D. 1986, MNRAS, 220, 1047
Courvoisier, T. J. L., Walter, R., Rodriguez, J., Bouchet, L., & Lutovinov, A. A. 2003, IAUC, 8063, 3
de Plaa, J., den Hartog, P. R., Kaastra, J. S., in't Zand, J. J. M., Mendez, M., & Hermsen, W. 2003, ATel, 119, 1
Filliatre, P., & Chaty, S. 2004, ApJ, 616, 469
Hill, A. B., Walter, R., Knigge, C., et al. 2005, A&A, 439, 255
Howk, J. C., Cassinelli, J. P., Bjorkman, J. E., & Lamers, H. J. G. L. M. 2000, ApJ, 534, 348
in't Zand, J. J. M. 2005, A&A, 441, L1
Jain, C., Paul, B., & Dutta, A. 2009, MNRAS, 397, L11
Kaplan, D. L., Moon, D. S., & Reach, W. T. 2006, ApJ, 649, L107
Kaur, R., Wijnands, R., Patruno, A., et al. 2009, MNRAS, 394, 1597
Kuulkers, E. 2005, AIPC, 797, 402
Kuulkers, E., Shaw, S. E., Paizis, A., et al. 2007, A&A, 466, 595
Lebrun, F., Leray, J. P., Lavocat, P., et al. 2003, A&A, 411, L141
Levine, A. M., & Corbet, R. 2006, ATel, 940, 1
Liu, Q. Z., van Paradijs, J., & van den Heuvel, E. P. J. 2000, A&AS, 147, 25
Liu, Q. Z., van Paradijs, J., & van den Heuvel, E. P. J. 2006, A&A, 455, L1165
Lutovinov, A., Revnivtsev, M., Gilfanov, M., Shtykovskiy, P., Molkov, S., & Sunyaev, R. 2005, A&A, 444, 821
Masetti, N., Mason, E., Morelli, L., et al. 2008, A&A, 482, 113
Matt, G., & Guainazzi, M. 2003, MNRAS, 341, L13
Negueruela, I., Smith, D. M., Reig, P., Chaty, S., & Torrejon, J. M. 2006, ESASP, 604, 165
Negueruela, I., Torrejon, J. M., Reig, P., Ribo, M., & Smith, D. M. 2008, AIPC, 1010, 252
Press, W. H., & Rybicki, G. B. 1989, ApJ, 338, 277
Rahoui, F., Chaty, S., Lagage, P., & Pantin, E. 2008, A&A, 484, 801
Revnivtsev, M. G., Sazonov, S. Yu., Gilfanov, M. R., & Sunyaev, R. A. 2003, AstL, 29, 587
Revnivtsev, M. G., Sunyaev, R. A., Varshalovich, D. A., et al. 2004, AstL, 30, 382
Romano, P., Sidoli, L., Mangano, V., Mereghetti, S., & Cusumano, G. 2007, A&A, 469, L5
Scargle, J. D. 1982, ApJ, 263, S835
Schartel, N., et al. 2003, IAUC, 8072, 3
Sguera, V., Barlow, E. J., Bird, A. J., et al. 2005, A&A, 444, 221
Sguera, V., Bazzano, A., Bird, A. J., et al. 2006, ApJ, 646, 452
Sguera, V., Hill, A. B., Bird, A. J., et al. 2007, A&A, 467, 249
Sidoli, L., Romano, P., Esposito, P., et al. 2009, arXiv:0907.4041
Sidoli, L., Romano, P., Mereghetti, S., Paizis, A., Vercellone, S., Mangano, V., & Gotz, D. 2007, A&A, 476, 1307
Ubertini, P., Lebrun, F., Di Cocco, G., et al. 2003, A&A, 411, L131
Walter, R., et al. 2003, A&A, 411, L427
Winkler, C., Courvoisier, T. J. L., Di Cocco, G., et al. 2003, A&A, 411, L1
Zurita Heras, J. A., de Cesare, G., Walter, R., Bodaghee, A., Belanger, G., Courvoisier, T. J. L., Shaw, S. E., & Stephen, J. B. 2006, A&A, 448, 261